International Journal of Solids and Structures 48 (2011) 592–602

Contents lists available at ScienceDirect

International Journal of Solids and Structures

journal homepage: www.elsevier.com/locate/ijsolstr

Single beam analysis of damaged beams verified using a strain energy based damage measure

A. Dixit *, S. Hanagud

Daniel Guggenhiem, School of Aerospace Engineering, Georgia Institute of Technology, 270 Ferst Drive, Atlanta, GA 30332-0150, United States

ARTICLE INFO

Article history:
Received 19 April 2009
Received in revised form 4 August 2010
Available online 30 October 2010

Keywords:
Structural health monitoring
Modal superposition method
Perturbation method
Single beam analysis
Damaged beams
Damage measure
Notch shaped damage

ABSTRACT

Analytical expression of a new damage measure which relates the strain energy, to the damage location and magnitude, is presented in this paper. The strain energy expression is calculated using modes and natural frequencies of damaged beams that are derived based on single beam analysis considering both decrease in mass and stiffness. Decrease in mass and stiffness are a fallout of geometric discontinuity and no assumptions regarding the physical behavior of damage are made. The method is applicable to beams, with notch like non-propagating cracks, with arbitrary boundary conditions. The analytical expressions derived for mode shapes, curvature shapes, natural frequencies and an improved strain energy based damage measure, are verified using experiments. The improvement in the damage measure is that it is not assumed that the bending stiffness of the damaged beam is constant, and, equal to that of undamaged beam when calculating the strain energy of the entire beam. It is also not assumed that the bending stiffness of the element in which the damage is located is constant.

1. Introduction

Most of the literature in the area of Structural Health Monitoring (SHM), has been directed at developing methods to predict the damage location and the damage magnitude using dynamics based experimental measurements. There are some mathematical models, that give analytical theory to model the damage. Such mathematical models for structures with damage are useful in two ways, firstly; they allow understanding of the physics behind the problem, which helps in the explanation of experimental readings. Secondly, they allow prediction of response of the structure. These studies are also useful for the development of new experimental techniques. At a broad level, overviews of the approaches used for SHM can be found in Staszewski et al. (2004) and Doebling et al. (1998).

1.1. Mathematical models

Krawczuk (2002) used concepts of fracture mechanics to develop a mathematical model for cracked beams. Knowledge of K_I, K_{II} and K_{III} is required to apply the theory presented. Approximate methods were used by Christides and Barr (1984) who used the Rayleigh–Ritz method, Shen and Pierre (1990) who used the Galerkin Method, and Qian et al. (1991) who used Finite Element model to predict the behavior of a beam with an edge crack. Law and Lu (2005) used assumed modes and modeled the crack mathematically as a Dirac delta function. Wang and Qiao (2007) approximated the modal displacements using Heaviside's function which meant that modal displacements were discontinuous at the crack location.

Other ways in which the rectangular edge defect has been modeled are as a spring (Ismail et al., 1990), an elastic hinge (Ostachowicz and Krawczuk, 1991), a cut-out slot (Kirshmer, 1944) and a pair of concentrated moment couple (Thompson, 1949). It has also been modeled by Joshi as a zone with reduced Young's modulus (Joshi and Madhusudhan, 1991) and as Bilinear stiffness (Ballo, 1999). Crack function models were used by Chondros et al. (1998), while breathing cracks concept was used by Cheng et al. (1999) to model cracks.

Luo and Hanagud (1997) uniquely formulate an integral equation to model a structure with notch type damage, and, successfully demonstrate a solution technique using perturbation method. Their mathematical treatment of the damaged structures offers a theoretical means to perform the parametric studies on the damage location and size. Next Luo and Hanagud (1998) and subsequently Lestari (2001) have proposed a perturbation method to describe the behavior of damaged beams. Lestari has used Fourier sine series expansion for the modes of damaged beams with simply supported ends. While Sharma et al. (2005, 2008) "assumed the approximate solution" of the damaged plate in terms of the double Fourier sine series again for a plate simply supported on all four ends. However, both Lestari and Sharma did not obtain the complementary solution, but only the particular integral for the higher order equations.

* Corresponding author. Tel.: +1 404 385 2773; fax: +1 404 894 2760.
E-mail address: wilkn@yahoo.com (A. Dixit).

0020-7683/$ - see front matter © 2010 Elsevier Ltd. All rights reserved.
doi:10.1016/j.ijsolstr.2010.10.025

1.2. Damage measure using methods based on experiments

In early attempts, changes in the modal parameters such as natural frequencies, mode shapes (West, 1984), damping ratios (Modena et al., 1999), and frequency response functions (Schulz et al., 1998), due to structural defects, were associated with damage (Sohn et al., 2003).

Ho and Ewins (2000) formulated a "Damage Index" defined as the quotient squared of the corresponding modal curvatures of the undamaged and damaged structure. Foundation to this damage index is based on the use of curvature by other researchers like Luo and Hanagud (1997) and Pandey et al. (1991). Ma and Asundi (2001) demonstrate that it is possible to compute the curvature mode shapes through the use of longitudinal strains at the surface. Salawu and Williams (1993) demonstrate that not all curvature mode shapes are sensitive to damages. Luo and Hanagud (1999) show that it is possible to use Poli-Vinyl-Diene-Floride (PVDF) sensors directly to obtain signals that are proportional to the curvature.

Wang et al. (2000) proposed a different damage index that is related to energy criterion. This damage index is based on the work of Sohn et al. (2003) who showed that strain energy is extremely sensitive to damage. Kim et al. (1997) formulate a Damage Index without requiring the knowledge of the dynamic response of the undamaged structure. Shi et al. (2000) formulated a distributed parameter, Modal Strain Energy Change Ratio (MSECR), based on the ratio of the change in strain energy of each element to the original strain energy of that element. The stiffness of the element is kept the same for the undamaged as well as damaged structure for strain energy computations of both states of the structure. The quality of this indicator is improved by summing the contributions of multiple modes in a normalized fashion.

Choi and Stubbs (1997) gave another damage index based on strain energy ratios. A ratio of strain energy of each element with respect to all elements in the structure is formulated for the undamaged as well as the damaged structure. In Cornwell's (1999) paper the method is extended to two dimensional structures. However, in both the papers the ratio of stiffness of the undamaged to damaged beams or plates is the damage measure. This assumes that the beam stiffness over the entire length of undamaged and damaged beam or plate is same. Also it is assumed that for the damaged element, the damage extends to the entire element and therefore, bending stiffness can be taken out of the strain energy integral equation. These assumptions are not made in this paper when calculating the DM.

1.3. Overview

A general method to tackle problems, of; beams with rectangular notches, for any boundary conditions for which the modal superposition method is valid, is proposed in this paper. Instead of making assumptions regarding the physical behavior of the damage the actual differential equations are solved to arrive at the solution of modal displacements. The Perturbation method (Nayfeh, 1985) is used to attend to the inherent non-linearity.

The derived mode shapes and natural frequencies are used to relate the strain energy based damage index to the damage location and damage magnitude (length and depth of damage). At this stage only the damage location is determined but the process can be extended to determine the damage magnitude too. The damage index is independent of beam properties such as stiffness and mass per unit length. The results are validated by conducting experiments using piezo-electric actuators and non-contact Laser-Doppler Vibrometer sensors.

First in Section 1, a literature survey of the relevant aspects of the paper, namely, a mathematical model to obtain the mode shapes and natural frequencies of a damaged beam, and, a proposed Damage Measure (DM), is done. Next in Section 2 the procedure to obtain the mode shapes and natural frequencies of the damaged beam is given. A method to calculate a strain energy based DM measure is described in Section 3. The ability of the method to correctly predict the location of damage is verified, for beams with a variety of boundary conditions in Section 4. Some conclusions are discussed in Section 5.

2. Natural frequencies and modes of a damaged beam by method of perturbation

In deriving the modes and natural frequencies of damaged beam the following assumptions are made.

1. The neutral axis of the beam is assumed to be undistorted due to the damage.
2. The damage is not located at the supports.
3. Euler–Bernoulli beam assumptions are assumed to be valid.
4. Interaction effect which is a highly non-linear effect, and happens when crack tips touch each other during vibrations, is neglected in this paper.

The natural modes of vibration of Euler–Bernoulli beam are given by the equation

$$\frac{d^2}{dx^2}\left[E(x)I(x)\frac{d^2}{dx^2}\phi(x)\right] - m(x)\lambda\phi(x) = 0 \tag{1}$$

where $E(x)$ and $I(x)$ are the Young's modulus and area moment of inertia at a section 'x' of the beam, $m(x)$ is the Mass per unit length at the same section. λ is any constant independent of x and t.

Consider an uniform rectangular cross-section of width b and depth h as shown in Fig. 1. A damage is located at $x = x_d$ with an extent of Δl and depth of h_d. Therefore, at the damage location the depth of the beam is reduced to $h - h_d$. For a notch like damage, crack profile can be approximated by using Heaviside functions $H(x - x_d) - H(x - x_d - \Delta l)$. Then the sectional bending stiffness $EI(x)$ and sectional mass $m(x)$ for beam is given as

$$\begin{aligned} EI(x) &= \frac{Ebh(x)^3}{12} = \frac{Eb(h - h_d(x))^3}{12} \\ &= \frac{Ebh^3}{12}\left(1 - \frac{h_d}{h}(H(x - x_d) - H(x - x_d - \Delta l))\right)^3 \\ m(x) &= m_0\left(1 - \frac{h_d}{h}(H(x - x_d) - H(x - x_d - \Delta l))\right) \end{aligned} \tag{2}$$

Assuming Δl to be small, and therefore $H(x - x_d) - H(x - x_d - \Delta l) \approx \Delta l\delta(x - x_d)$ for sharp cracks (Law and Lu, 2005) where $\delta(x)$ is the dirac delta function. Expanding the above equation binomially and retaining only the term uptill order one in Δl the following expressions are obtained.

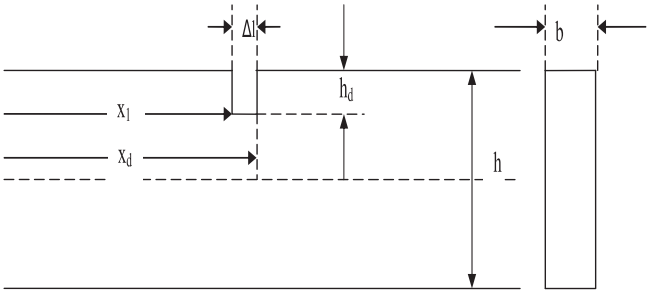

Fig. 1. Notched beam.

$$EI(x) \approx EI_0(1 - \epsilon\Delta l\delta(x - x_d)) \tag{3a}$$

$$m(x) \approx m_0\left(1 - \frac{1}{3}\epsilon\Delta l\delta(x - x_d)\right) \tag{3b}$$

$$\epsilon = \frac{3h_d}{h} \tag{3c}$$

In the above equation I_0 and m_0 are nominal quantities at an undamaged location. As the quantity ϵ is small, the function $\phi(x)$ and λ are expanded using perturbation theory (Nayfeh, 1985) as the following series

$$\begin{aligned}\phi(x) &= \phi(x)^0 - \epsilon\phi(x)^1 - \epsilon^2\phi(x)^2 - \cdots \\ \lambda &= \lambda^0 - \epsilon\lambda^1 - \epsilon^2\lambda^2 - \cdots\end{aligned} \tag{4}$$

The superscripts of ϕ and λ denote the order of perturbation. Eqs. (3a), (3b) and (4) are substituted in (1) to give

$$\begin{aligned}&\frac{d^2}{dx^2}\left[EI_0(1 - \epsilon\Delta l\delta(x - x_d))\left(\frac{d^2}{dx^2}\left(\phi(x)^0 - \epsilon\phi(x)^1 - \epsilon^2\phi(x)^2\right)\right)\right] \\ &\quad - m_0\left(1 - \frac{1}{3}\epsilon\Delta l\delta(x - x_d)\right)\left(\lambda^0 - \epsilon\lambda^1 - \epsilon^2\lambda^2\right)\left(\phi(x)^0 - \epsilon\phi(x)^1 - \epsilon^2\phi(x)^2\right) \\ &\quad = 0\end{aligned} \tag{5}$$

The equations of order 0, 1 and 2 in ϵ are obtained as

$$\epsilon^0 : EI_0\frac{d^4\phi^0}{dx^4} - \lambda^0 m_0\phi^0 = 0 \tag{6a}$$

$$\begin{aligned}\epsilon^1 : EI_0\frac{d^4\phi^1}{dx^4} - \lambda^0 m_0\phi^1 &= \lambda^1 m_0\phi^0 + \frac{1}{3}\lambda^0 m_0\phi^0\Delta l\delta(x - x_d) \\ &\quad - EI_0\Delta l\frac{d^2}{dx^2}\left[\delta(x - x_d)\frac{d^2\phi^0}{dx^2}\right]\end{aligned} \tag{6b}$$

$$\begin{aligned}\epsilon^2 : EI_0\frac{d^4\phi^2}{dx^4} - \lambda^0 m_0\phi^2 &= \lambda^2 m_0\phi^0 - \lambda^1 m_0\phi^1 - \frac{1}{3}\lambda^0 m_0\phi^1\Delta l\delta(x - x_d) \\ &\quad - \frac{1}{3}\lambda^1 m_0\phi^0\Delta l\delta(x - x_d) + EI_0\Delta l\frac{d^2}{dx^2}\left[\delta(x - x_d)\frac{d^2\phi^1}{dx^2}\right]\end{aligned} \tag{6c}$$

A quantity 'a' is defined such that $a^4 = \frac{m_0\lambda^0}{EI_0}$. In general, the beam is supported with different boundary conditions, however, Eq. (6a) is same as equation for modal vibrations of undamaged beam. Let the solution to the equation be given by

$$\begin{aligned}&\lambda^0 = \lambda_n^0, \quad n = 1, 2, 3, \ldots, \infty \\ &\phi^0(x) = \phi_n^0(x), \quad n = 1, 2, 3, \ldots, \infty\end{aligned} \tag{7}$$

Using the condition of orthogonality, the following two equations are obtained

$$\int_0^L EI\left(\phi_m^0\right)''\left(\phi_n^0\right)''dx = \lambda^0\int_0^L m_0\left(\phi_m^0\right)\left(\phi_n^0\right)dx = \delta_{mn}Q_{mn} \tag{8}$$

where δ_{mn} is the Kronecker delta and Q_{mn} is a constant. Next the Eq. (6b) is solved. Eq. (6b) is different from (6a) as it has a RHS. Hence the total solution consists of an homogeneous part and a particular integral part $\left(\phi_n^1 = \phi_n^1|_{homogeneous} + \phi_n^1|_{particular}\right)$. The only unknown in the RHS of (6b) is λ_n^1. Homogeneous part of equation yields $\phi_n^1|_{homogeneous} = \phi_n^0$ since the homogeneous part of both (6a) and (6b) is same. The particular solution, $\phi_n^1|_{particular}$ is expanded in terms of the orthogonal modes ϕ_k^0

$$\phi_n^1|_{particular} = \sum_{k=1}^{\infty}\eta_{nk}\phi_k^0 \tag{9}$$

From Eqs. (6b), (9) and (7) we obtain the following equation (one for each mode of vibration for the beam) given below:

$$\begin{aligned}EI_0\sum_{k=1}^{\infty}\eta_{nk}\left(\phi_k^0\right)'''' - \lambda_n^0 m_0\sum_{k=1}^{\infty}\eta_{nk}\phi_k^0 &= \lambda_n^1 m_0\phi_n^0 + \frac{1}{3}\lambda_n^0 m_0\Delta l\delta(x - x_d)\phi_n^0 \\ &\quad - EI_0\Delta l\frac{d^2}{dx^2}\left[\delta(x - x_d)\left(\phi_n^0\right)''\right]\end{aligned} \tag{10}$$

Multiplying Eq. (10) by $\phi_j^0(x)$, integrating from $x = 0$ to $x = L$, we get

$$\begin{aligned}&\sum_{k=1}^{\infty}\eta_{nk}\left(EI_0\int_0^L\left(\phi_k^0\right)''''\phi_j^0dx - \lambda_n^0 m_0\int_0^L\phi_k^0\phi_j^0dx\right) = \lambda_n^1 m_0 \\ &\quad\times\int_0^L\phi_n^0\phi_j^0dx + \frac{1}{3}\lambda_n^0 m_0\Delta l\int_0^L\delta(x - x_d)\phi_n^0\phi_j^0dx - EI_0\Delta l \\ &\quad\times\int_0^L\frac{d^2}{dx^2}\left[\delta(x - x_d)\left(\phi_n^0\right)''\right]\phi_j^0dx\end{aligned} \tag{11}$$

The integrals in Eq. (11) are evaluated as follows:

$$m_0\int_0^L\phi_n^0\phi_j^0dx = \delta_{nj}Q_{nj} \tag{12a}$$

$$\int_0^L\delta(x - x_d)\phi_n^0\phi_j^0dx = \phi_n^0(x_d)\phi_j^0(x_d) \tag{12b}$$

$$\begin{aligned}\int_0^L\frac{d^2}{dx^2}\left[\delta(x - x_d)\left(\phi_n^0\right)''\right]\phi_j^0dx &= \frac{d}{dx}\left[\delta(x - x_d)\left(\phi_n^0\right)''\right]\phi_j^0\Big|_0^L \\ &\quad - \left[\delta(x - x_d)\left(\phi_n^0\right)''\right]\left(\phi_j^0\right)'\Big|_0^L \\ &\quad + \int_0^L\left[\delta(x - x_d)\left(\phi_n^0\right)''\right]\left(\phi_j^0\right)''dx \\ &= \left(\phi_n^0(x_d)\right)''\left(\phi_j^0(x_d)\right)''\end{aligned} \tag{12c}$$

Notice the first two terms (12c) are zero because $\delta(x - x_d) = 0$ at both $x = L$, and $x = 0$. The first integral on the lhs of (11) is simplified as

$$\begin{aligned}\sum_{k=1}^{\infty}\eta_{nk}EI_0\int_0^L\left(\phi_k^0\right)''''\phi_j^0dx &= \sum_{k=1}^{\infty}\left(\eta_{nk}EI_0\left(\left(\phi_k^0\right)'''\phi_j^0\Big|_0^L - \left(\phi_k^0\right)''\left(\phi_j^0\right)'\Big|_0^L\right.\right. \\ &\quad \left.\left. + \int_0^L\left(\phi_k^0\right)''\left(\phi_j^0\right)''dx\right)\right)\end{aligned} \tag{13}$$

The boundary terms go to zero since the eigen function satisfy the boundary conditions. Using (8) the above equation is written as

$$EI_0\eta_{nj}\int_0^L\left(\left(\phi_j^0\right)''\right)^2dx = \lambda_j^0 m_0\eta_{nj}\int_0^L\left(\phi_j^0\right)^2dx \tag{14}$$

Similarly the second term of lhs of (11) can be simplified using (8). The lhs of (11) is transformed as

$$\eta_{nj}m_0\int_0^L\left(\left(\phi_j^0\right)\right)^2dx\left(\lambda_j^0 - \lambda_n^0\right) \tag{15}$$

The expression $m_0\int_0^L\left(\phi_j^0\right)^2dx$ in the above equation is denoted by m_{0j}. Eq. (11) can now be written as

$$\begin{aligned}\eta_{nj}m_{0j}\lambda_j^0 - \lambda_n^0 m_{0j}\eta_{nj} &= \lambda_n^1 m_0\delta_{nj}Q_{nj} + \frac{1}{3}\lambda_n^0 m_0\Delta l\phi_n^0(x_d)\phi_j^0(x_d) \\ &\quad - EI_0\Delta l\left(\phi_n^0(x_d)\right)''\left(\phi_j^0(x_d)\right)''\end{aligned} \tag{16}$$

For $j = n$, the lhs becomes zero and hence

$$\lambda_n^1 = \frac{\Delta l \lambda_n^0}{\int_0^L \left(\phi_n^0\right)^2 dx}\left(\frac{\left(\left(\phi_n^0(x_d)\right)''\right)^2}{a^4} - \frac{1}{3}\left(\phi_n^0(x_d)\right)^2\right) \tag{17}$$

For $n \neq j$

$$\eta_{nj} = \frac{\Delta l}{\frac{\lambda_j^0}{\lambda_n^0} - 1}\frac{\frac{1}{3}\phi_n^0(x_d)\phi_j^0(x_d) - \frac{1}{a^4}\left(\phi_n^0(x_d)\right)''\left(\phi_j^0(x_d)\right)''}{\int_0^L \left(\phi_j^0\right)^2 dx} \tag{18}$$

$$\phi_n^1 = \phi_n^0 + \sum_{j=1, j\neq n}^{\infty} \eta_{nj}\phi_j^0 \tag{19}$$

The second order correction is required for calculation of strain energy. The same procedure is used to solve Eq. (6c). The second order correction quantities are obtained as

$$\lambda_n^2 = \frac{\Delta l \lambda_n^0}{\int_0^L \left(\phi_n^0\right)^2 dx}\left(\frac{\left(\left(\phi_n^0(x_d)\right)''\right)^2}{a^4} - \frac{1}{3}\phi_n^0(x_d)\phi_n^1(x_d) - \frac{\lambda_n^1}{3\lambda_n^0}\phi_n^1(x_d)\phi_n^0(x_d)\right) \tag{20}$$

$$\beta_{nl} = \frac{\Delta l}{\frac{\lambda_l^0}{\lambda_n^0} - 1}\frac{\frac{1}{a^4}\left(\phi_n^0(x_d)\right)''\left(\phi_j^0(x_d)\right)'' - \frac{1}{3}\phi_n^1(x_d)\phi_l^0(x_d) - \frac{\lambda_n^1}{3\lambda_n^0}\phi_n^0(x_d)\phi_l^1(x_d)}{\int_0^L \left(\phi_l^0\right)^2 dx} \tag{21}$$

$$\phi_n^2 = \phi_n^0 + \sum_{l=1, l\neq n}^{\infty} \beta_{nl}\phi_l^0 \tag{22}$$

Finally, the natural frequency and mode shape correct to the order 2 for a damaged beam is given by

$$\phi_n = \phi_n^0 - \epsilon\left[\phi_n^0 + \sum_{j=1, j\neq n}^{\infty} \eta_{nj}\phi_j^0\right] - \epsilon^2\left[\phi_n^0 + \sum_{l=1, l\neq n}^{\infty} \beta_{nl}\phi_l^0\right], \tag{23a}$$

$$\lambda_n = \lambda_n^0 - \epsilon\lambda_n^1 - \epsilon^2\lambda_n^2. \tag{23b}$$

Plots of modes shapes and curvature for damaged and undamaged beams correct till first order of perturbation are given in Figs. 2 and 3. A detailed discussion about the Figures is given in the results section.

3. Strain energy based damage measure in terms of damage parameters

The strain energy due to bending, for the undamaged beam, excited in its nth mode is given as

$$U_n = \frac{1}{2}a_n^2\int_0^L EI(x)\left((\phi_n)''\right)^2 dx. \tag{24}$$

The strain energy for the undamaged beam is given by U_{ud}

$$U_{ud} = U_n = \frac{1}{2}a_n^2\int_0^L EI_0\left((\phi_n)''\right)^2 dx. \tag{25}$$

Similarly the strain energy due to bending, of the damaged beam U_d can be calculated by substituting (3a) and (23a) in (24). Therefore

$$U_d = \frac{1}{2}a_n^2\int_0^L EI_0(1 - \epsilon\Delta l\delta(x - x_d))\left(\left(\phi_n^0 - \epsilon\left[\phi_n^0 + \sum_{j=1, j\neq n}^{\infty}\eta_{nj}\phi_j^0\right] - \epsilon^2\left[\phi_n^0 + \sum_{l=1, l\neq n}^{\infty}\beta_{nl}\phi_l^0\right]\right)''\right)^2 dx. \tag{26}$$

Collecting terms up to the order of 2 in ϵ

$$U_d = \frac{1}{2}a_n^2\int_0^L EI_0(1 - \epsilon\Delta l\delta(x - x_d))\left(\left(\left(\phi_n^0\right)''\right)^2 - 2\epsilon\left(\phi_n^0\right)''\left[\left(\phi_n^0\right)'' + \sum_{j=1, j\neq n}^{\infty}\eta_{nj}\left(\phi_j^0\right)''\right] + \epsilon^2\left[\left(\phi_n^0\right)'' + \sum_{j=1, j\neq n}^{\infty}\eta_{nj}\left(\phi_j^0\right)''\right]^2 - 2\epsilon^2\left(\phi_n^0\right)''\left[\left(\phi_n^0\right)'' + \sum_{l=1, l\neq n}^{\infty}\beta_{nl}\left(\phi_l^0\right)''\right]\right)dx \tag{27}$$

The above equation is further simplified by using the condition of orthogonality

$$U_d = \frac{1}{2}a_n^2\int_0^L EI_0\left(\left(\phi_n^0\right)''\right)^2 - 2\epsilon\left(\left(\phi_n^0\right)''\right)^2 + \epsilon^2\left[\left(\left(\phi_n^0\right)''\right)^2 + \sum_{j=1, j\neq n}^{\infty}\eta_{nj}^2\left(\left(\phi_j^0\right)''\right)^2\right] - 2\epsilon^2\left(\left(\phi_n^0\right)''\right)^2 dx - \epsilon\Delta l\frac{1}{2}a_n^2 EI_0\left[\left(\left(\phi_n^0(x_d)\right)''\right)^2 - 2\epsilon\left(\phi_n^0(x_d)''\right)^2 + \epsilon^2\left[\left(\left(\phi_n^0(x_d)\right)''\right)^2 + \sum_{j=1, j\neq n}^{\infty}\eta_{nj}^2\left(\left(\phi_j^0(x_d)''\right)\right)^2\right]\right] \tag{28}$$

A way to calculate damage measure, based on strain energy is given in Cornwell (1999). It is measured by calculating the change in flexural rigidity of a sub-region of the beam. For this, the beam is divided into several sub-divisions. The Damage Measure for the kth segment is given by D_{Mk}

$$D_{Mk} = \frac{(EI)_k}{(EI)_k^*} = \left\{\frac{\int_{a_k}^{a_{k+1}}\left(\frac{\partial^2\phi_i^*}{\partial x^2}\right)^2 dx}{\int_0^L\left(\frac{\partial^2\phi_i^*}{\partial x^2}\right)^2 dx}\right\}\Big/\left\{\frac{\int_{a_k}^{a_{k+1}}\left(\frac{\partial^2\phi_i}{\partial x^2}\right)^2 dx}{\int_0^L\left(\frac{\partial^2\phi_i}{\partial x^2}\right)^2 dx}\right\}, \tag{29}$$

where the starred quantities denote the quantities with damage, and a_k denotes the starting coordinate of the kth division. An advantage of the above representation is that, the modes need not be normalized and, the constant associated with displacement is canceled. However, an important assumption made in the above derivation is that the flexural rigidity of the whole beam is same for damaged beam and undamaged beam, and that the flexural rigidity of the damaged beam element is reduced to a constant. In other words, the damage is assumed to extend to the whole damaged segment. Mathematically this translates in taking out the non constant $EI(x)$ term out of the integral in (24) for both the segment strain energy and strain energy for the whole beam. Obviously this cannot be mathematically justified. Hence, here it is proposed that the flexural rigidity term be retained inside the integral. This is possible because we have been able to analytically obtain the expressions of mode shapes of a damaged beam as shown above. Substituting flexural rigidity from (3a) and formula for damaged mode shape from (23a), the following expression is obtained

$$U_d = EI_0\left[(1 - 2\epsilon - \epsilon^2)\int_0^L\left(\left(\phi_n^0\right)''\right)^2 dx + \epsilon^2\left(\int_0^L\sum_{j=1, j\neq n}^{\infty}\eta_{nj}^2\left(\left(\phi_j^0\right)''\right)^2 dx\right) - \epsilon\Delta l\left(\left(\phi_n^0(x_d)\right)''\right)^2 - 2\epsilon\left(\phi_n^0(x_d)''\right)^2\right] \tag{30}$$

Damage Measure D_M is then be calculated by

$$D_M = \frac{U_{di}}{U_d}\Big/\frac{U_{udi}}{U_{ud}} \tag{31}$$

The subscript 'i' denotes the strain energy for the ith segment (x_i to x_{i+1}), U_{di} and U_{udi} are given by

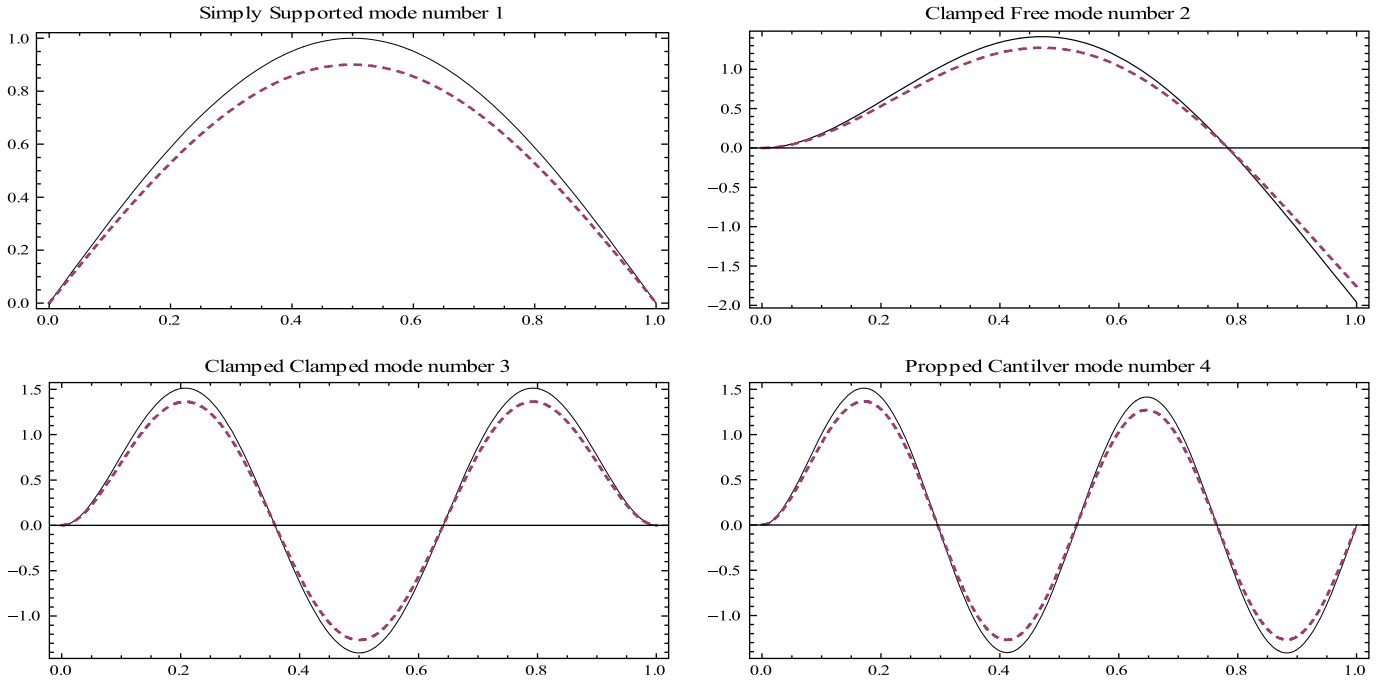

Fig. 2. Damaged (dashed lines) and undamaged (continuous lines) mode shapes, $x_d = 0.35L$, $\Delta l = 0.01L$, $\epsilon = 0.1/3$.

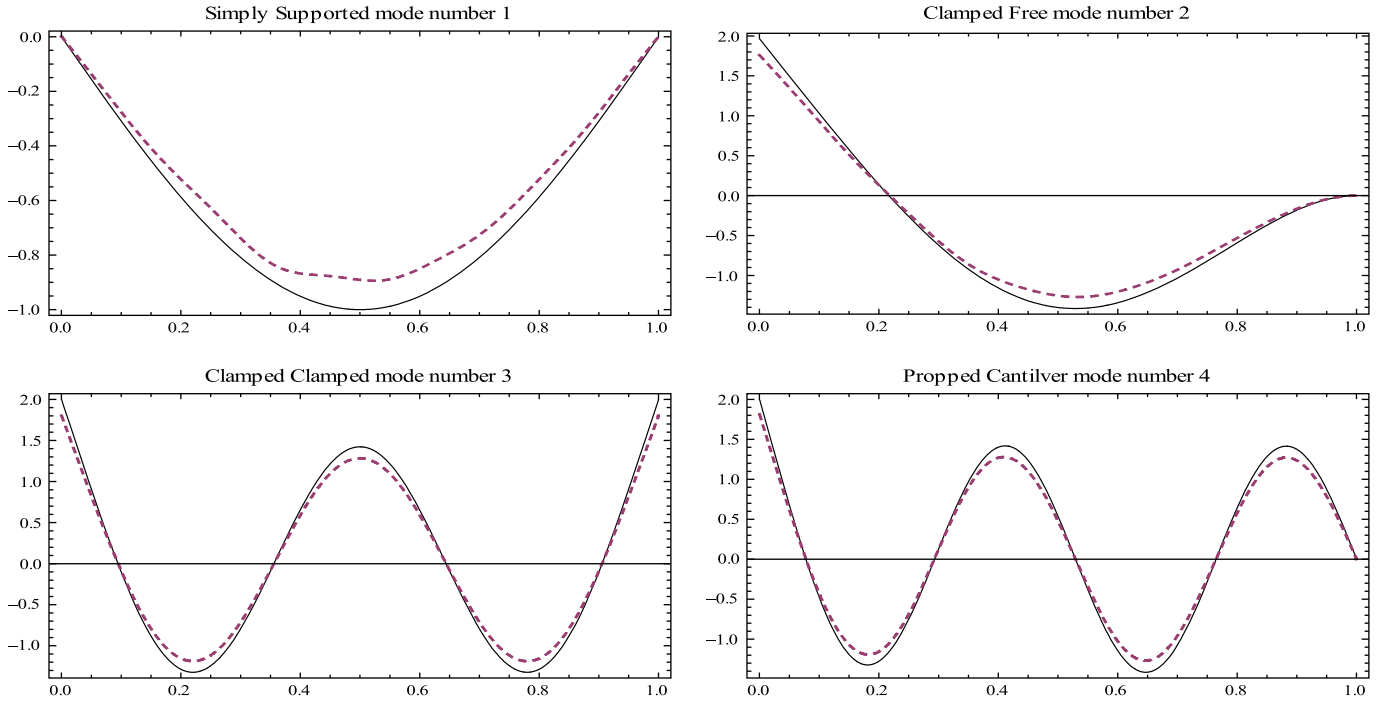

Fig. 3. Damaged (dashed lines) and undamaged (continuous lines) curvature shapes, $x_d = 0.35L$, $\Delta l = 0.01L$, $\epsilon = 0.1/3$.

$$U_{di} = EI_0(1-2\epsilon-\epsilon^2)\left[\int_{x_i}^{x_{i+1}} \left((\phi_n)''\right)^2 + \sum_{j=1,j\neq n}^{\infty} \frac{\epsilon^2\eta_{nj}^2}{1-2\epsilon-\epsilon^2} \times\left(\left(\phi_j^0\right)''\right)^2 - \frac{\delta(x-x_d)\Delta l\epsilon(1-2\epsilon)}{1-2\epsilon-\epsilon^2}\left(\left(\phi_n^0(x_d)\right)''\right)^2\right] \tag{32}$$

$$U_{udi} = \int_{x_i}^{x_{i+1}} EI_0\left((\phi_n)''\right)^2 dx$$

$$U_d = EI_0(1-2\epsilon-\epsilon^2)\left[\int_0^L \left((\phi_n)''\right)^2 dx + \int_0^L \sum_{j=1,j\neq n}^{\infty} \times\frac{\epsilon^2\eta_{nj}^2}{1-2\epsilon-\epsilon^2}\left(\left(\phi_j^0\right)''\right)^2 dx - \frac{\Delta l\epsilon(1-2\epsilon)}{1-2\epsilon-\epsilon^2}\left(\left(\phi_n^0(x_d)\right)''\right)^2\right] \tag{33}$$

$$\phi_n = (1-2\epsilon-\epsilon^2)\left(\phi_n^0 - \sum_{j=1,j\neq n}^{\infty} \frac{\eta_{nj}\epsilon}{1-2\epsilon-\epsilon^2}\phi_j^0\right)$$

Attention is now drawn to Eqs. (23a) and (30) which give the damaged mode shape and strain energy. The expressions are reproduced below in a changed form

Let the expression $\sum_{j=1,j\neq n}^{\infty} \frac{\eta_{nj}\epsilon}{\sqrt{1-2\epsilon-\epsilon^2}}\phi_j^0$ be denoted by $\Gamma(x,damage)$ or global damage sensitivity function and $\frac{\Delta l\epsilon(1-2\epsilon)}{(1-2\epsilon-\epsilon^2)}\left(\left(\phi_n^0(x_d)\right)''\right)^2$ by

$\Lambda(damage)$ or local damage sensitivity constant. The argument 'damage' in the expressions denote the damage parameters $(x_d, \epsilon, \Delta l)$. The above expressions can now be simplified to

$$U_d = U_{ud} + EI_0 \int_0^L \left((\Gamma(x, damage)'')^2 dx \right) - EI_0 \Lambda(damage)$$
$$\phi_n = \phi_n^0 - \Gamma(x, damage) \tag{34}$$

It can be seen that the displacements exhibit global sensitivity to damage through the function $\Gamma(x,damage)$ only while strain energy has both global and an acute local sensitivity to damage through the function $\Gamma(x,damage)$ and through the constant $\Lambda(damage)$, respectively. Another important observation is that the strain energy is increased everywhere except at damage location where it is reduced due to local damage sensitivity constant.

4. Results and verification

4.1. Analytical results

To show the generic nature of the theory presented, four types of beams (Simply Supported (SS), Clamped Free (CF) Clamped Clamped (CC) and Propped Cantilever (PC)) are considered. First, in Fig. 2, the damaged mode shape (dashed line) is given for each beam. The first damaged mode is given for SS beam, second of CF beam, third for CC beam and fourth of PC beam. For the figure $x_d = 0.35L$, $\Delta l = 0.01L$, $\epsilon = 0.1/3$. The damaged modes are given along side the undamaged modes (continuous line). Similarly in Fig. 3 the damaged curvature shapes are given (same modes and same beams) along side undamaged curvature. It is seen that mode profiles of damaged and undamaged beams are similar and the damage cannot be identified just by looking at the mode profiles.

Next in Fig. 4, the damage measure derived is calculated for the beams. Again the same trend is followed as previous figures as far as beams and their mode numbers are concerned. It is observed that the location of damage is clearly identified using the damage measure. The noticeable features of the plot are that there is an uniform global effect of damage all along the beams since the magnitude of damage measure is greater than one. However, at the damage location there is an acute localized drop. Hence, strain energy measure gives a direct visual information regarding location of damage. It seems likely to be able to give damage parameters too due to the localized damage effect. Similar discontinuity at the damage location was experimentally observed by Cornwell (1999). Another interesting observation regarding the plots is that the drop at damage location is directly proportional to the increase at non damage locations. There is a compensating effect evident in these plots.

The next Fig. 5 gives the plot of damage measure vs. the mode number for all the four types of beams. It is observed that, the sensitivity of damage measure to damage is dependent on the mode number. Some modes are more sensitive to damage than others. To normalize this erratic behavior cumulative damage measure has been used by researchers. Cumulative damage measure is an average of the damage measure over a number of modes. Cumulative damage measure is used from this point on.

The cumulative damage measures for different depth of damage to total depth ratio is given in next figure, Fig. 6. Finally cumulative damage measure is given for different extent of damages in Fig. 7. The results of last two Figs. 6 and 7 are on expected lines since the magnitude of damage has a direct bearing on DM. The Δl value is more sensitive to damage than ϵ value. The results go as per intuition but it should be kept in mind that there is an inherent limit on the value of ϵ as per the theory. According the theory Neutral Axis is assumed to remain unaffected by the damage. Also there is a limit on Δl value since the notch shaped defect given by Heaviside function was approximated by a sharp crack given by a dirac delta function.

4.2. Experimental verification

Experiments were conducted to verify the theory using the experimental setup given in Fig. 8. Polytec (TM) SDLV was used

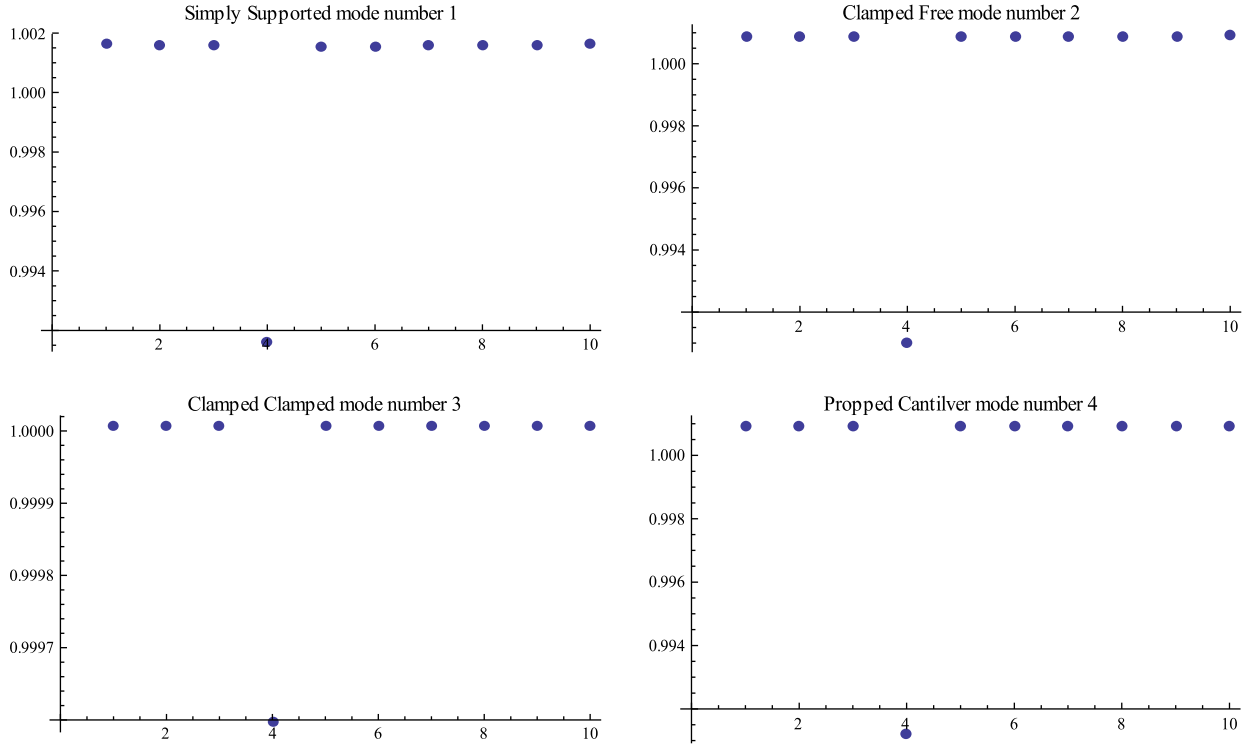

Fig. 4. Damaged measure, Eq. (31), $x_d = 0.35L$, $\Delta l = 0.01L$, $\epsilon = 0.1/3$.

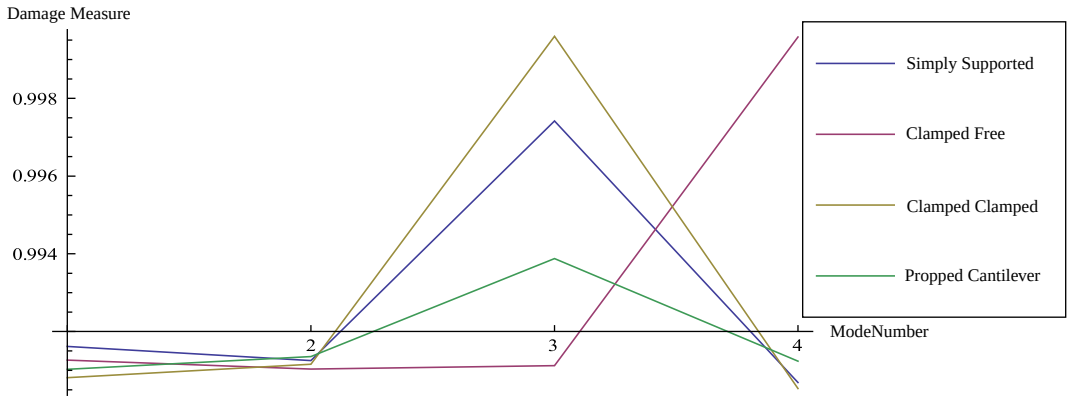

Fig. 5. Damage measures for modes (1–4) at $x_d = 0.35L$, $\Delta l = 0.01L$, $\epsilon = 0.1/3$.

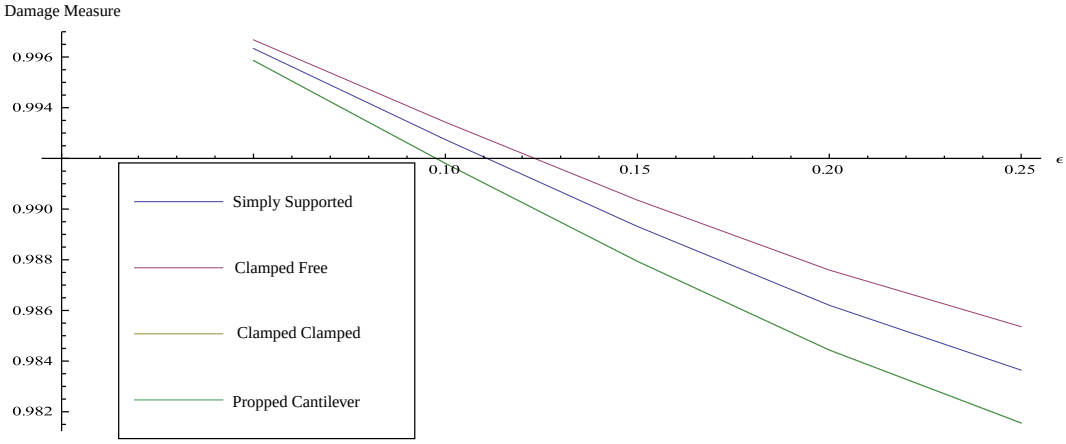

Fig. 6. Effect of ϵ on damage measure, $x_d = 0.35L$, $\Delta l = 0.01L$.

to generate an input voltage. The signal generated (4 V) by the SDLV was amplified 100 times by an amplifier. A broadband white noise was used as the input excitation. A piezoelectric actuator was fixed towards the clamped end of the beam to provide the input excitation. Frequencies up to 2 kHz were excited. Low pass signal filtering was used. A grid consisting of 105 points was used for an undamaged beam. For the damaged beam 505 points were used to take the readings. More points were used for the damaged case to be able to see any minute changes in mode shapes and curvature shapes at the damage location. The resonance frequencies where the Frequency Response Function (FRF) Fig. 9 reached the peak amplitudes and also the phase change was 180°, were retained as modal frequencies. The other sharp peaks, other than the peaks for natural frequencies are the harmonics of the power signal, since

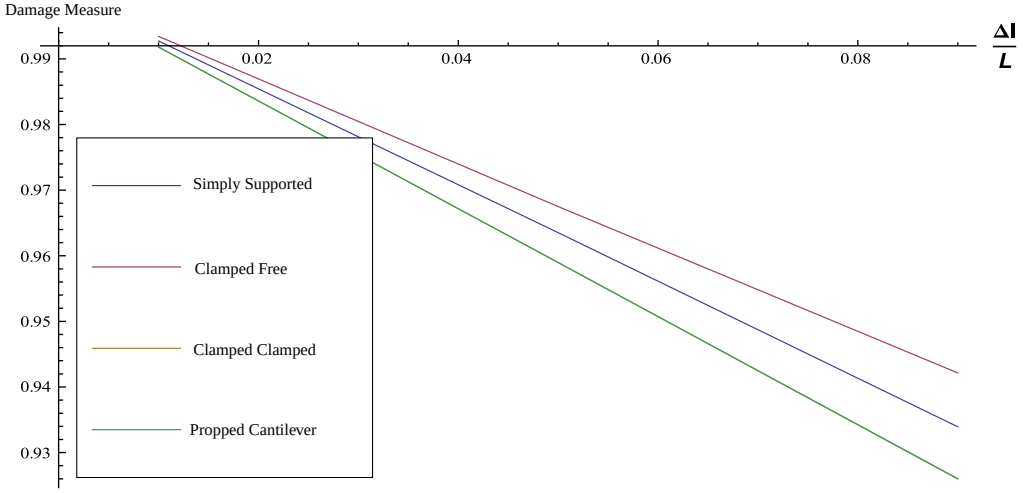

Fig. 7. Effect of Δl on damage measure, $x_d = 0.35L$, $\epsilon = 0.1/3$.

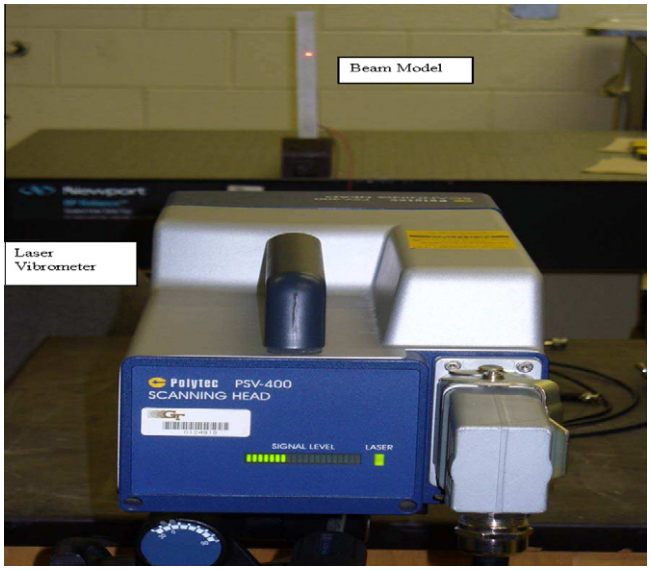

Fig. 8. Experimental setup.

they occur at multiples of 60 Hz. 10 readings were taken with remeasure option being switched on. Data acquisition was done using Polytec (TM) data acquisition software. The obtained modal data, in universal file format, was processed using an in-house developed software. The average was taken for the points across the beam to simulate the beam neutral axis. Curve fitting was done to get a continuous curve for the Operating Deflected Shape (OSD). OSD was assumed to be equivalent to the mode shape for this experiment.

The results presented in the paper were verified by doing experiments on a cantilever beam. A fiber glass beam was used for the purpose. Modes were calculated experimentally for both damaged and undamaged beam. A rectangular notch shaped damage was made at 0.35 the length of the beam ($x_d = 0.35L$). The damage was 0.1 the depth ($\epsilon = 0.3$), and the notch length was 0.05 the length of the beam ($\Delta l = 0.05L$). The Young's modulus for the beam was 29 GPa, density of the beam 3749 kg/m^3, the length 0.267 m, the moment of inertia 1.28e10^{-10} m^4 and area 10^{-4} m^2.

In Table 1 the analytical and experimental values for natural frequencies of the beam are given. The experiments show close correlation to analytical values for lower modes, for higher modes the difference in the readings increases. The experimental setup had to be dismantled for making the notch after the readings on

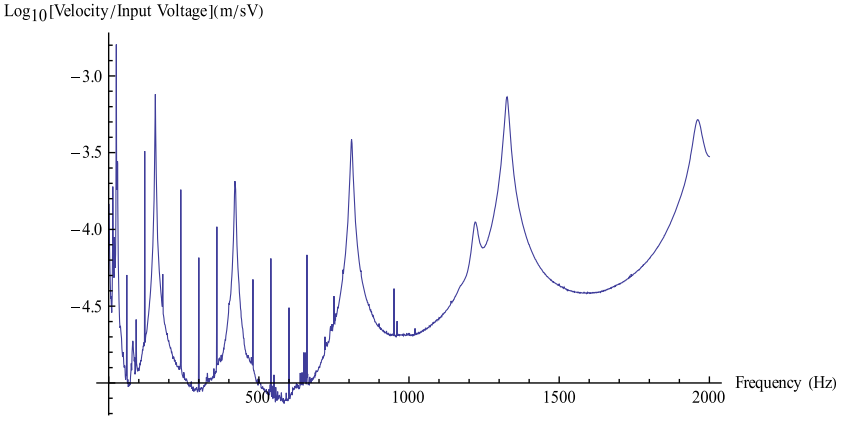

Fig. 9. Frequency response function, averaged velocity (m/s) against frequency (Hz).

Table 1
Frequency results comparison analytical vs. experimental (Hz).

Mode	Experimental		Analytical		$\%\text{error} = \frac{Dam_{anal} - Dam_{expt}}{Dam_{anal}}$
	Undamaged $Undam_{expt}$	Damaged Dam_{expt}	Undamaged $Undam_{anal}$	Damaged Dam_{anal}	
1	25.6	25	24.9	24.3	2.88
2	153	155	156	154.6	0.26
3	419	420	436.7	427.8	4.16
4	809	801	855.7	855.7	6.39
5	1314	1326	1414.6	1382.6	4.09

Table 2
Frequency results comparison (Hz) with Law and Lu (2005) Table 2 (law), Eq. (23b) (dixit) $x_d = 0.381$, $\Delta l = 0.005$.

Mode	$\epsilon = 0$		$\epsilon = 0.16$		$\epsilon = 0.32$		$\epsilon = 0.48$	
	Law	Dixit	Law	Dixit	Law	Dixit	Law	Dixit
2	22.86	22.43	22.80	22.43	22.77	22.42	22.77	22.42
3	62.76	62.81	62.62	62.80	62.38	62.80	62.89	62.80
4	123.05	123.08	122.56	122.85	121.70	122.62	120.0	122.40
5	203.24	203.46	202.27	202.91	201.05	202.36	198.49	201.81
6	303.45	303.93	302.49	303.45	301.51	302.97	299.5	302.49

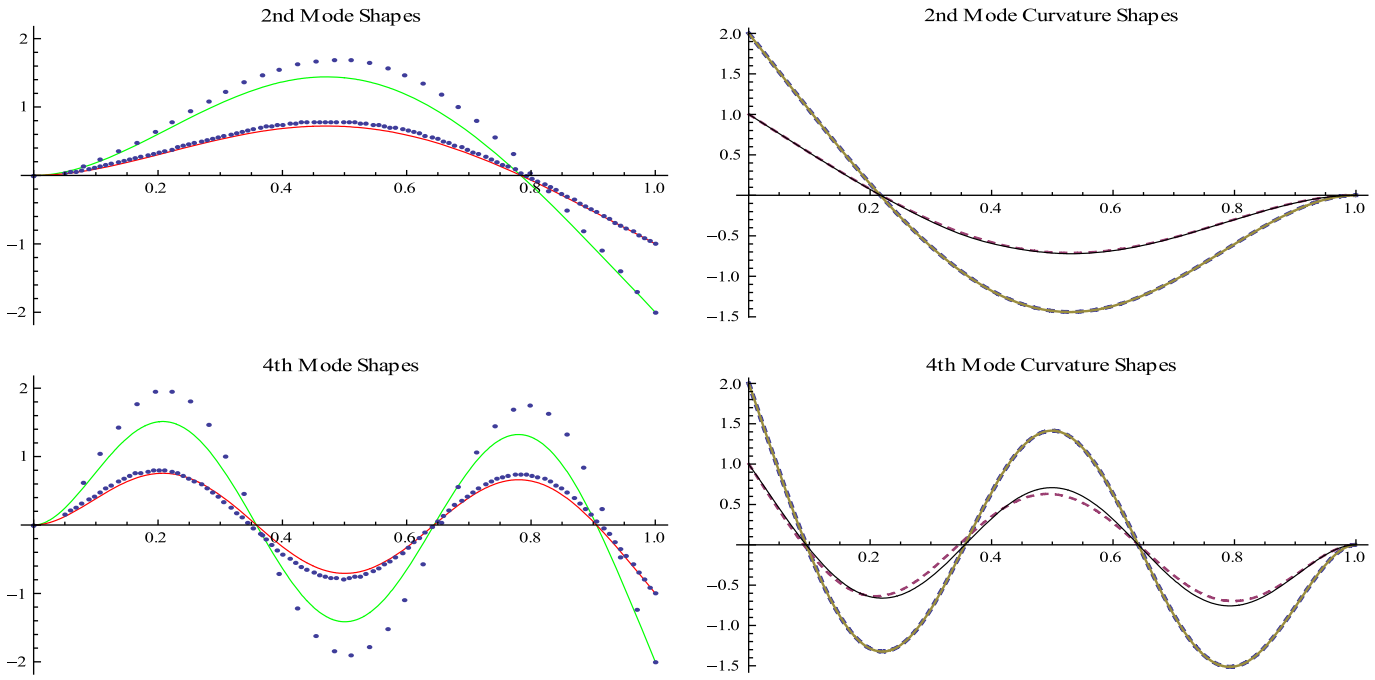

Fig. 10. Modes and curvature of undamaged (normalized to 2) and damaged (normalized to 1) beam for experimental mode shapes (dots), experimental curve fitted curvatures (dashed lines), analytical mode shapes and curvatures (continuous lines).

the undamaged beam. The end conditions therefore may change and the readings may get affected. To further validate the derivation using results from published work, the natural frequency values given by Law and Lu (2005) in Table 2 are compared with analytical values from Eqs. (23b), (20) and (17). The Table 2 of Law et al. is reproduced for easy reference. The saw width is given to be 1.3 mm, accounting for the kerf and material loss, the extent of damage is estimated to be ($\Delta l = 0.005$) as deduced from the thickness of the blade used to make the saw cut. The position of damage was ($x_d = 0.38$). Natural frequency values for three values of ϵ, $\epsilon = 0.16$, 0.32, 0.48 are given in the paper. The Young's Modulus $E = 207$ GPa, mass density $\rho = 7832$ kg/m^3, area $A = 4.75\text{e}10^{-4}$ m^2 and area moment of inertia $I = 1.43\text{e}10^{-8}$ m^4. The comparison is given in Table 2. The maximum percentage difference in the values is 2%. A point to note is that Law et al. missed the first natural frequency and the values provided are from 2nd to 6th rather than 1st to 5th as claimed. This can be easily ascertained by looking at the first undamaged frequency value which comes out to be 3.58 Hz. Looking at the values of the natural frequencies it can be said that the presence of damage is indicated by change of natural frequency but its location and magnitude cannot be directly ascertained.

In Fig. 10, the modes and curvature shapes for experimental and analytical, damaged and undamaged beam are shown. Two modes, mode 2 and 4 are plotted. In the mode shapes curve; the dots are the experimental data, and the continuous lines give the analytical data. The experimental data was curve fitted. The experimental curve fitted curvatures are given in the curvature plot as dashed lines, the analytical curvature plots are given by continuous lines. The damaged beam mode shape and curvature shapes are normalized to 1 and undamaged beam mode shape and curvature to 2. Also the damage measure calculation again for modes one through four is given in Fig. 11. The dashed line gives the experimental value of the damage measure and the black line for the theoretical

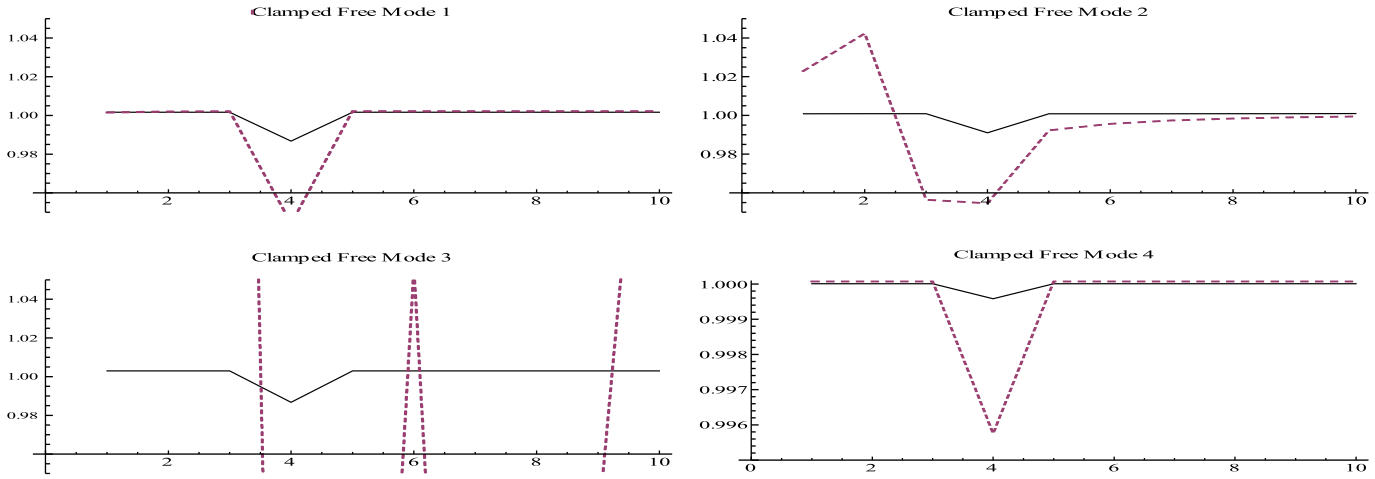

Fig. 11. Damage measure for clamped free beam, dashed (experimental), solid (analytical).

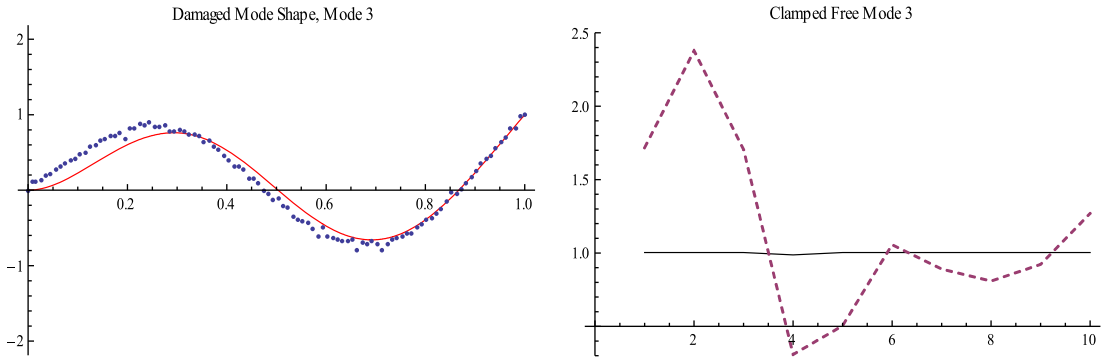

Fig. 12. Mode shape, dots (experimental data), continuous line (analytical) for clamped free beam 3rd mode, damage measure, dashed (experimental), solid (analytical).

values. The modes shape 2, which is more sensitive to damage, shows a disturbance at the place of the actuator attachment to the beam. This can be attributed to the additional mass provided by the actuator. Mode 3 has an unique phenomenon occurring, as the natural frequency value coincided with the natural harmonics of the power supply (420 Hz). As a result there was experimental noise in the measurement of the mode shape. The damage measure values still showed the indication of damage, but the correlation with analytical values was lost. Fig. 12 shows the third mode shape of the damaged beam along with the damage measure values at a different scale than as shown in Fig. 11.

5. Discussion of results and conclusions

A procedure to calculate the mode shapes and natural frequencies for damaged beams in terms of modes and natural frequencies of undamaged beam and damage parameters like location and magnitude of damage, is given. Single beam analysis without any assumptions regarding the physical behavior of damage is used. This was verified by using natural frequencies (Tables 1 and 2), mode and curvature shapes (Figs. 2, 3 and 10) and an improved strain energy based damage measure (Figs. 4 and 11) The procedure was shown to be applicable to beams with different end conditions.

It was seen that the damaged and undamaged modes shapes and curvature shapes were similar and it was difficult to ascertain the position of the damage using them.

Regarding the natural frequencies, a change in their value indicates the presence of damage, however they were not able to directly give the location of damage nor its magnitude. The change in natural frequencies is given by $\epsilon\lambda_n^1$, where λ_n^1 is given by Eq. (17). It is seen in the equation that decrease in mass increases the natural frequency and decrease in stiffness decreases it. The change in the natural frequency is an aggregate effect consisting of these two mutually contradicting effects, so the natural frequency cannot serve as a robust indicator of the magnitude of the damage. The change in mass effect, which has been neglected by many researchers was successfully considered in this paper. In some damages where there is no change in mass like delamination, the change in mass can be neglected, but in other damages, like damages due to corrosion and erosion, this effect should be accounted for.

The veracity of the theory presented was further ascertained using an improved damage measure based on strain energy. The damage measure was shown to be extremely sensitive to the damage as both the discontinuity in stiffness and also the curvature are contained in the damage measure. A limitation of the damaged measure was that it depended on accurate measurement of damaged mode shapes. Two damage parameters one giving global damage influence $\Gamma(x,damage)$ and another giving acute local damage influence $\Lambda(damage)$ were discovered. Since Λ(damage) is a function of damage magnitude (ϵ and Δl), the damage measure can be used to find the damage magnitude. This is a topic for further study by the authors.

References

Ballo, I., 1999. Non-linear effects of vibration of a continuous transverse cracked slender shaft. Journal of Sound and Vibration 217 (2), 321–333.
Cheng, S.M., Swamidas, A.S.J., Wu, X.J., Wallace, W., 1999. Vibrational response of a beam with a breathing crack. Journal of Sound and Vibration 225 (3), 201–208.
Choi, S., Stubbs, N., 1997. Nondestructive damage detection algorithms for 2d plates. In: Smart Systems for Bridges, Structures, and Highways, Proceedings of SPIE, vol. 3.
Chondros, T., Dimarogonas, A., Yao, J., 1998. A continuous cracked beams vibration theory. Journal of Sound and Vibration 215 (1), 17–34.
Christides, S., Barr, A.D.S., 1984. One-dimensional theory of cracked Euler–Bernoulli beams. International Journal of Mechanical Sciences 26 (11–12), 339–348.
Cornwell, P., 1999. Application of the strain energy damage detection method to plate-like structures. Journal of Sound and Vibration 224 (2), 359–374.
Doebling, S., Farrar, C.R., Prime, M., 1998. Summary review of vibration-based damage identification methods. Shock and Vibration Digest 30, 91–105.
Ho, Y., Ewins, D., 2000. Numerical evaluation of the damage index. In: Structural Health Monitoring 2000. Stanford University, pp. 995–1011.
Ismail, F., Ibrahim, A., Martin, H.K., 1990. Identification of fatigue cracks from vibration testing. Journal of Sound and Vibration 140, 305–317.
Joshi, A., Madhusudhan, B.S., 1991. A unified approach to free vibration of locally damaged beams having various homogeneous boundary conditions. Journal of Sound and Vibration 147, 475–488.
Kim, K., Ryu, J., Lee, S., Choi, L., 1997. In-situ monitoring of Sungsan bridge in Han river with a optical fiber sensor system. In: Smart Systems for Bridges, Structures, and Highways, Proceedings of SPIE, vol. 1.
Kirshmer, P.G., 1944. The effect of discontinuities on the natural frequency of the beam. In: Proceedings of ASTM, vol. 44, pp. 897–904.
Krawczuk, M., 2002. Application of spectral beam finite element with a crack and iterative search technique for damage detection. Finite Elements in Analysis and Design 9–10, 991–1004.
Law, S., Lu, Z.R., 2005. Crack identification in beam from dynamic responses. Journal of Sound and Vibration 285, 967–987.
Lestari, W., 2001. Damage of Composite Structures: Detection Technique, Dynamic Response and Residual Strength. Ph.D. Thesis, Georgia Institute of Technology, School of Aerospace Engineering.
Luo, H., Hanagud, S., 1997. An integral equation for changes in the structural characteristics of damaged structures. International Journal of Solids and Structures 34, 4557–4579.
Luo, H., Hanagud, S., 1998. Detection of debonding in thermal protective system titles by using nonlinear structural dynamic response. In: Structural Dynamics, and Materials Conference, an Exhibit.
Luo, H., Hanagud, S., 1999. PVDF film sensor and its application in damage detection. Journal of Aerospace Engineering 12 (1), 23–30.
Ma, J., Asundi, A., 2001. Structural health monitoring using a fiber optic polarimetric sensor and a fiber optic curvature sensor static and dynamic test. Smart Materials and Structures 10, 181–188.
Modena, C., Sonda, D., Zonta, D., 1999. Damage localization in reinforced concrete structures by using damping measurements. In: Proceedings of the International Conference on Damage Assessment of Structures, DAMAS 99, pp. 132–141.
Nayfeh, A., 1985. Problems in Perturbation. Wiley, New York.
Ostachowicz, W., Krawczuk, M., 1991. Analysis of the effect of cracks on the natural frequencies of a cantilever beam. Journal of Sound and Vibrations 150, 191–201.

Pandey, A., Biswas, M., Samman, M., 1991. Damage detection from changes in curvature mode shapes. Journal of Sound and Vibration 145 (2), 321–332.
Qian, G.L., Gu, S.N., Jiang, J.S., 1991. The dynamic behavior and crack detection of a beam with a crack. Journal of Sound and Vibration 138, 233–243.
Salawu, O., Williams, C., 1993. Structural damage detection using experimental modal analysis – a comparison of some methods. In: Proceedings of 11th International Modal Analysis Conference, pp. 254–260.
Schulz, M., Naser, A., Thyagarajan, S., Mickens, T., Pai, P., 1998. Structural health monitoring using frequency response functions and sparse measurements. In: Proceedings of the International Modal Analysis Conference, pp. 760–766.
Sharma, V., 2008. Damage Index Estimation in Beams and Plates Using Laser Vibrometry. Ph.D. Thesis, Georgia Institute of Technology, School of Aerospace Engineering.
Sharma, V., Hanagud, S., Ruzzene, M., 2005. Damage index estimation in beams and plates using laser vibrometry. In: Proceedings of the 2005 International Workshop on Structural Health Monitoring.
Shen, M.H., Pierre, C., 1990. Natural modes of Euler–Bernoulli beams with symmetric cracks. Journal of Sound and Vibration 138, 115–134.
Shi, Z.Y., Law, S.S., Zhang, L.M., 2000. Structural damage detection from modal strain energy change. Journal of Engineering Mechanics 126 (12), 1216–1223.
Sohn, H., Farrar, C.R., Hemez, F.M., Shunk, D.D., Stinemates, D.W., Nadler, B.R., 2003. A Review of Structural Health Monitoring Literature: 1996-2001, Los Alamos National Laboratory Report, LA-13976-MS.
Staszewski, W., Boller, C., Tomlinson, G., 2004. Health Monitoring of Aerospace Structures: Smart Sensor Technologies and Signal Processing. John Wiley and Sons, Inc., England.
Thompson, W.T., 1949. Vibration of slender bars with discontinuities in stiffness. Journal of Applied Mechanics 16, 203–207.
Wang, J., Qiao, P., 2007. Vibration of beams with arbitrary discontinuities and boundary conditions. Journal of Sound and Vibration 308 (1–2), 12–27.
Wang, M., Xu, F., Lloyd, G., 2000. A systematic numerical analysis of the damage index method used for bridge diagnostics. In: Smart Structures and Materials 2000: Smart Systems for Bridges, Structures and Highways, Proceedings of SPIE, vol. 3, pp. 154–164.
West, W., 1984. Illustration of the use of modal assurance criterion to detect structural changes in an orbiter test specimen. In: Proceedings of the Air Force Conference on Aircraft Structural Integrity, pp. 1–6.